

First Estimate of the Primary Cosmic Ray Energy Spectrum above 3 EeV from the Pierre Auger Observatory

The Pierre Auger Collaboration

Presenter: P. Sommers (sommers@physics.utah.edu)

Measurements of air showers are accumulating at an increasing rate while construction proceeds at the Pierre Auger Observatory. Although the southern site is only half complete, the cumulative exposure is already similar to those achieved by the largest forerunner experiments. A measurement of the cosmic ray energy spectrum in the southern sky is reported here. The methods are simple and robust, exploiting the combination of fluorescence detector (FD) and surface detector (SD). The methods do not rely on detailed numerical simulation or any assumption about the chemical composition.

Introduction

The southern site of the Pierre Auger Cosmic Ray Observatory in Argentina now covers an area of approximately 1500 km². On good-weather nights, air fluorescence telescopes record the longitudinal profiles of extensive air showers in the atmosphere above the surface array of water Cherenkov detectors [2, 3]. Hybrid air shower measurements (FD and SD together) are utilized in this analysis to avoid dependence on specific numerical simulations of air showers and detector responses to them. The analysis is also free of assumptions about the primary nuclear masses. The fluorescence detector (FD) provides a nearly calorimetric, model-independent energy measurement: fluorescence light is produced in proportion to energy dissipation by a shower in the atmosphere [4]. Hybrid data establish the relation of shower energy to the ground parameter $S(1000)$, which is the water Cherenkov signal in the SD at a distance of 1000 meters from the shower axis. Moreover, hybrid data determine the trigger probability for individual tanks as a function of core distance and energy, from which it is found that the SD event trigger is fully efficient above 3 EeV for zenith angles less than 60°. The SD exposure is then calculated simply by integrating the geometric aperture over time.

It is the continuously operating surface array which provides the high statistics with unambiguous exposure.

The methods adopted for this first analysis are chosen to be robust and simple. No event-by-event estimation of shower penetration is attempted, although a variety of methods to achieve that may improve the energy resolution in future reports. The rapidly growing cumulative exposure will provide much higher statistics for future measurements of the spectrum. Besides the present statistical uncertainties, the presentation here also takes account of unresolved systematic uncertainties.

Analysis methods and results

The data for this analysis are from 1 Jan 2004 through 5 Jun 2005. The event acceptance criteria and exposure calculation are described in separate papers [5, 6]. Events are included for zenith angles 0-60°, and results are reported for energies above 3 EeV (3525 events). The array is fully efficient for detecting such showers, so the acceptance at any time is the simple geometric aperture. The cumulative exposure adds up to 1750 km² sr yr, which is 7% greater than the total exposure obtained by AGASA [1]. The average array size during the time of this exposure was 22% of what will be available when the southern site of the Observatory has been completed.

Assigning energies to the SD event set is a two-step process. The first step is to assign an energy parameter S_{38} to each event. Then the hybrid events are used to establish the rule for converting S_{38} to energy.

The energy parameter S_{38} for each shower comes from its experimentally measured $S(1000)$, which is the time-integrated water Cherenkov signal $S(1000)$ that would be measured by a tank 1000 meters from the core.

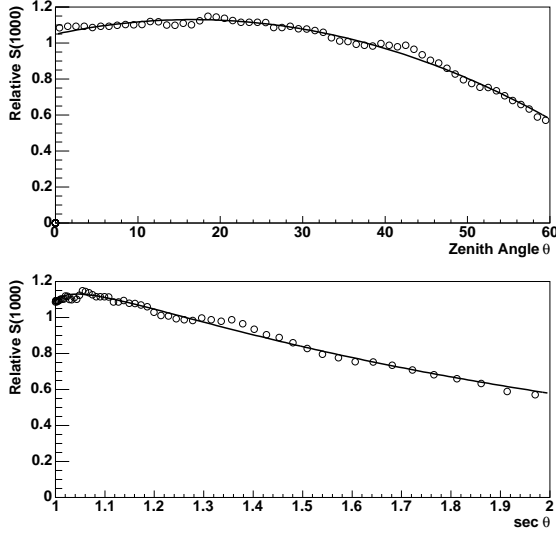


Figure 1. The constant intensity curve $CIC(\theta)$ is determined by having the same number of events for $\sin\theta\cos\theta\Delta\theta = 0.1$ at each θ (plotted points are not independent). Values are relative to $S(1000)$ at the median zenith angle of 38° . The approximating quadratic curve is $CIC(\theta) = 1.049 + 0.00974\theta - 0.00029\theta^2$. In the lower plot, the CIC curve is replotted as a function of $\sec\theta$ to exhibit the attenuation of $S(1000)$ with atmospheric slant depth at fixed energy.

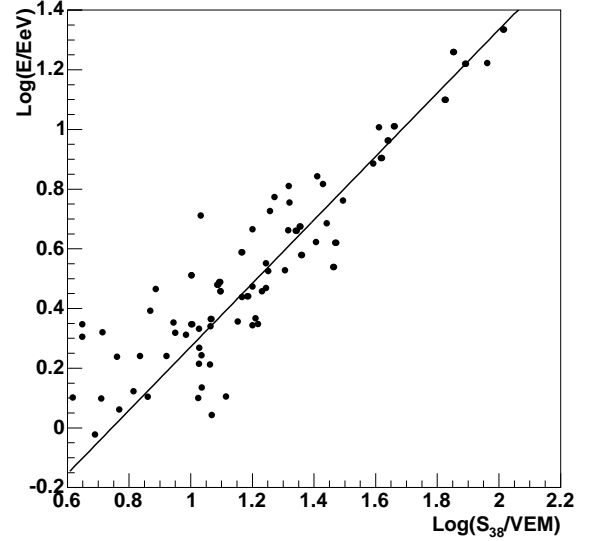


Figure 2. FD energy vs. ground parameter S_{38} . These are hybrid events that were recorded when there were contemporaneous aerosol measurements, whose FD longitudinal profiles include shower maximum in a measured range of at least 350 g cm^{-2} , and in which there is less than 10% Cherenkov contamination. The fitted line is $\text{Log}(E) = -0.79 + 1.06\text{Log}(S_{38})$.

This ground parameter is determined accurately by non-linear interpolation even when there is no tank at that particular core distance [7].

The slant depth of the surface array varies from 870 g cm^{-2} for vertical showers to 1740 g cm^{-2} for showers at zenith angle $\theta = 60^\circ$. The signal $S(1000)$ is attenuated at large slant depths. Its dependence on zenith angle is derived empirically by exploiting the nearly isotropic intensity of cosmic rays. By fixing a specific intensity I_0 (counts per unit of $\sin^2\theta$), one finds for each zenith angle the value of $S(1000)$ such that $I(> S(1000)) = I_0$. A particular constant intensity cut gives the curve $CIC(\theta)$ of figure 1. The $S(1000)$ values are shown relative to the value at the median zenith angle ($\theta \approx 38^\circ$). Given $S(1000)$ and θ for any measured shower, the energy parameter S_{38} is defined by $S_{38} \equiv S(1000)/CIC(\theta)$. It may be regarded as the $S(1000)$ measurement the shower would have produced if it had arrived 38° from the zenith.

This formula for S_{38} implicitly assumes that all constant intensity curves are simple rescalings of the reference curve $CIC(\theta)$ of figure 1, which corresponds to $S_{38} = 15 \text{ VEM}$ (vertical equivalent muons). Higher values of S_{38} also yield curves of constant intensity to the accuracy that can be checked with current statistics. With a much larger data set, it will be possible to investigate any change in shape of the constant intensity curve with energy and thereby reduce any systematic error that might be associated with this simple formula for S_{38} .

S_{38} is well correlated with the FD energy measurements in hybrid events that are reconstructed independently by the FD and SD. See figure 2. The fitted line gives an empirical rule for assigning energies (in EeV) based

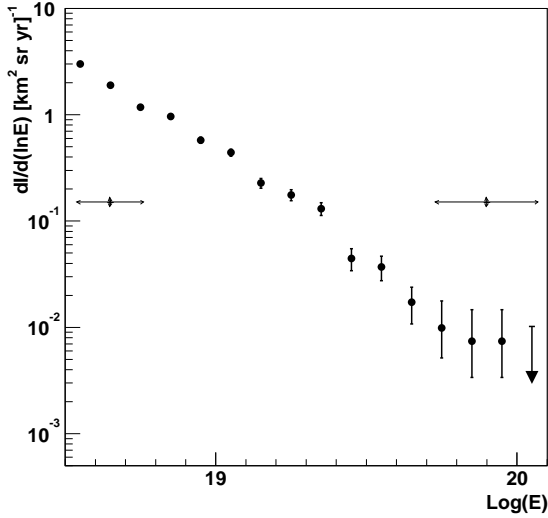


Figure 3. Estimated spectrum. Plotted on the vertical axis is the differential intensity $\frac{dI}{d \ln E} \equiv E \frac{dI}{dE}$. Error bars on points indicate statistical uncertainty (or 95% CL upper limit). Systematic uncertainty is indicated by double arrows at two different energies.

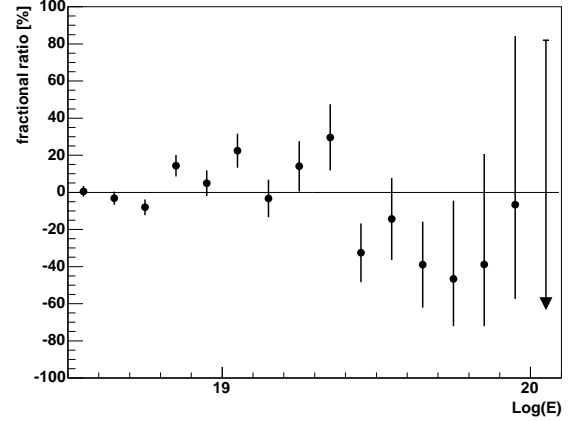


Figure 4. Percentage deviation from the best-fit power law: $100 \times ((dI/d(\ln E) - F)/F)$. The fitted function is $F = 30.9 \pm 1.7 \times (E/EeV)^{-1.84 \pm 0.03}$. The chisquare per degree of freedom in the fit is 2.4

on S_{38} (in VEM):

$$E = 0.16 \times S_{38}^{1.06} = 0.16 \times [S(1000)/CIC(\theta)]^{1.06}. \quad (1)$$

The uncertainty in this rule is discussed below. The hybrid events in figure 2 start at ~ 1 EeV. The acceptance is not saturated below 3 EeV, but the events used in figure 2 are those with core locations and arrival directions such that they have probability greater than 0.9 for satisfying the SD trigger and quality conditions. These events increase the statistics and the “moment arm” of the correlation without introducing appreciable bias.

The distribution over $\ln(E)$ produced by this two-step procedure becomes the energy spectrum of figures 3 and 4 after dividing by the exposure: $1750 \text{ km}^2 \text{ sr yr}$. (See also <http://www.auger.org/icrc2005/spectrum.html>.)

Uncertainties and caveats

The Auger Observatory will measure the spectrum over the southern sky accurately in coming years. The spectrum in figure 3 is only a first estimate. It has significant systematic and statistical uncertainties. The indicated statistical error for each point comes directly from the Poisson uncertainty in the number of measured showers in that logarithmic energy bin. Systematic and statistical uncertainties in $S(1000)$ are discussed elsewhere [8]. There is larger systematic uncertainty in the conversion of S_{38} to energy. Part of that comes from the FD energies themselves. Laboratory measurements of the fluorescence yield are uncertain by 15%, and the absolute calibration of the FD telescopes is presently uncertain by 12%. Together with other smaller FD uncertainties, the total systematic uncertainty in the FD energy measurements is estimated to be 25%. Another part of the systematic energy uncertainty in this analysis comes from quantifying the correlation in figure 2. The accuracy is limited by the available statistics, and the uncertainty grows with energy. Combining in quadrature the FD systematic uncertainty and this correlation uncertainty, the total systematic energy uncertainty grows from 30% at 3 EeV to 50% at 100 EeV. This uncertainty is indicated by horizontal double arrows in figure 3, and a 10% systematic uncertainty in the exposure is indicated by vertical arrows.

The fraction of primary energy that does not contribute to fluorescence light (due to neutrinos, muons, and other weakly interacting particles) has an estimated uncertainty of 4% due to the unknown primary mass and differences in viable hadronic interaction models. This is included in the 25% uncertainty for FD energies. It should be acknowledged, however, that it is not possible empirically to rule out larger amounts of “missing energy” due to exotic particle physics. In principle, some shower energies could be underestimated.

The spectrum of figure 3 is based on the water Cherenkov signal $S(1000)$. Primary photons would be expected to produce a smaller $S(1000)$ signal due to the lack of muons. On average, the $S(1000)$ from a photon primary should be roughly one-half the signal for a hadronic primary of the same energy. The Auger Observatory will eventually obtain upper limits on the photon flux at all energies. For now, the limit [9] does not pertain to the highest energies, so the results in figure 3 in the highest energy bins are predicated on the assumption that primary photons are not a major component.

Discussion and a look to the future

The Pierre Auger Observatory is still under construction and growing rapidly. By the next ICRC meeting, its cumulative exposure will be approximately 7 times greater. The statistical errors will shrink accordingly, permitting a search in the southern skies for spectral features, including the predicted GZK suppression. The enlarged hybrid data set will reduce systematic uncertainty in the FD normalization of the SD energies.

Numerous laboratory experiments are attempting to reduce the systematic uncertainty in the fluorescence yield, which will be the dominant uncertainty in the FD normalization of the Auger energy spectrum. The FD detector calibration uncertainty will also be reduced.

Preliminary studies based on comparing real data with simulation data give energies that are systematically higher than the FD-normalized energies by approximately 25%. This number has some dependence on the hadronic model, the primary mass and the shower propagation code that are assumed. The Pierre Auger Observatory is uniquely configured for the investigation of this intriguing difference. Measurements of X_{\max} , LDF steepness, signal rise time, and shower front curvature complement the measurement of $S(1000)$. Studying the distributions of these shower properties at different zenith angles and energies can constrain the cosmic ray composition and hadronic interaction models. The parameters might be used shower-by-shower to improve the accuracy of energy determinations. Future measurements of the energy spectrum will be based on vastly larger data sets and may also exploit the rich information that is available for each shower.

References

- [1] M. Takeda et al., *Astroparticle Physics* **19**, 447-462 (2003)
- [2] Auger Collaboration, *NIM* **523**, 50 (2004)
- [3] “Hybrid performance of the Pierre Auger Observatory,” usa-mostafa-M-abs1-he14-oral
- [4] “Performance of the fluorescence detectors of the Pierre Auger Observatory,” aus-bellido-J-abs1-he14-oral
- [5] “The trigger system of the PAO surface detector: operation, efficiency and stability,” usa-bauleo-PM-abs1-he14-poster
- [6] “Determination of the aperture of the PAO surface detector,” fra-parizot-E-abs1-he14-poster
- [7] “Measurement of the lateral distribution function of UHECR air showers,” usa-bauleo-PM-abs2-he14-poster
- [8] “Statistical and systematic uncertainties in the event reconstruction and $S(1000)$ determination by the Pierre Auger surface detector,” ita-ghia-P-abs1-he14-oral
- [9] “Upper limit on the primary photon fraction from the Pierre Auger Observatory,” ger-risse-M-abs2-he14-oral